Acta Biochimica Polonica

Vol. 50 No. 4/2003

909–920

QUARTERLY

Effects of distortions by A-tracts of promoter B-DNA spacer region on the kinetics of open complex formation by *Escherichia coli* RNA polymerase

Iwona K. Kolasa*, Tomasz Łoziński and Kazimierz L. Wierzchowski✉

Institute of Biochemistry and Biophysics, Polish Academy of Sciences, Warszawa, Poland

Received: 11 August, 2003; revised: 15 October, 2003; accepted: 03 December, 2003

Key words: kinetics of open complex formation, *Escherichia coli* RNA polymerase, DNA bending, A-tract, promoter spacer region, RNA polymerase–promoter interaction

A-tracts in DNA due to their structural morphology distinctly different from the canonical B-DNA form play an important role in specific recognition of bacterial upstream promoter elements by the carboxyl terminal domain of RNA polymerase α subunit and, in turn, in the process of transcription initiation. They are only rarely found in the spacer promoter regions separating the –35 and –10 recognition hexamers. At present, the nature of the protein–DNA contacts formed between RNA polymerase and promoter DNA in transcription initiation can only be inferred from low resolution structural data and mutational and crosslinking experiments. To probe these contacts further, we constructed derivatives of a model Pa promoter bearing in the spacer region one or two A_n (n = 5 or 6) tracts, in phase with the DNA helical repeat, and studied the effects of thereby induced perturbation of promoter DNA structure on the kinetics of open complex (RPo) formation *in vitro* by *Escherichia coli* RNA polymerase. We found that the overall second-order rate constant k_a of RPo formation, relative to that at the control promoter, was strongly reduced by one to two orders of magnitude only when the A-tracts were located in the nontemplate strand. A particularly strong 30-fold down effect on k_a was exerted by nontemplate A-tracts in the –10 extended promoter region, where an involvement of nontemplate TG (–14, –15) sequence in a specific interaction with region 3 of σ-sub-

*Present address: Department of Molecular Pathology, Institute of Oncology, W. Roentgena 5, 02-781 Warszawa, Poland.

✉Corresponding author: Kazimierz L. Wierzchowski, Institute of Biochemistry and Biophysics, Polish Academy of Sciences, A. Pawińskiego 5a, 02-106 Warszawa, Poland; tel.: (48 22) 658 4729; fax: (48 22) 658 4636; e-mail address: klw@ibb.waw.pl

Abbreviations: αCTD, C-terminal domain of α subunit of RNA polymerase; A-tract, a run of 5 or 6 adenosine residues in DNA; BSA, bovine serum albumin; DTT, dithiothreitol; EMSA, electrophoretic mobility shift analysis; Eσ^{70} or R, *Escherichia coli* RNA polymerase holoenzyme; FDAI, fluorescence-detected abortive initiation; P, promoter; RNAP, prokaryotic RNA polymerase; RPo, open transcription complex; UP, upstream promoter region.

unit is postulated. A-tracts in the latter location caused also 3-fold slower isomerization of the first closed transcription complex into the intermediate one that precedes formation of RPo, and led to two-fold faster dissociation of the latter. All these findings are discussed in relation to recent structural and kinetic models of RPo formation.

A-tracts within the UP promoter element of bacterial promoters, upstream of the –35 recognition hexamer, are specifically recognized by CTD domains of cognate RNA polymerase α subunits (Estrem *et al.*, 1999; Yasuno *et al.*, 2001) owing to their structure different from that of B-DNA (MacDonald *et al.*, 2001). In a previous study (Kolasa *et al.*, 2002) we showed that an A_5-tract adjacent to position –36 within the proximal subsite of the UP element inserted into a model non-regulated *Escherichia coli* promoter Pa (cf. Fig. 1), irrespective of its location in the template or nontemplate strand, significantly accelerated the rate of open complex formation *in vitro* by cognate RNA polymerase. However, shifting such a tract in the template strand by two bases downstream, so that it partially overlapped the –35 hexamer, led to a 5-fold decrease in this rate, most probably owing to perturbation of specific interactions of this promoter element with region 4 of σ^{70} and the CTD domain of RNA polymerase (RNAP) α subunit (Estrem *et al.*, 1999; Chen *et al.*, 2003; Ross *et al.*, 2003). These experiments demonstrated that A-tracts can be used as structural probes of RNAP–DNA contacts in other promoter regions, in particular in the spacer separating the –35 and –10 elements, where their occurrence in natural promoters is rather rare (Travers, 1987). Therefore, in parallel experiments (Kolasa, 2001), the poorly known specific contacts between RNAP and promoter spacer DNA (Naryshkin *et al.*, 2000; Mekler *et al.*, 2002; Murakami *et al.*, 2002) were probed by inserting A_n (n = 5 or 6) bending tracts in the spacer region of the Pa promoter and investigating their effects on the kinetics of abortive transcription *in vitro*. It was observed that two phased A_6-tracts in the template strand of the Pa derivative called Pe, do not significantly affect kinetic parameters of transcription initiation, while the presence of two phased A_5-tracts in the same regions of the nontemplate strand of the Pa derivative named Pi, exert a strong down effect. This observation prompted us to resolve how each of these tracts contributes to the observed effect. For this purpose kinetic properties of two simpler analogues of Pi bearing single A_6-tracts immediately downstream of the –35 hexamer (Pi35) and upstream of the –10 hexamer (Pi10) were

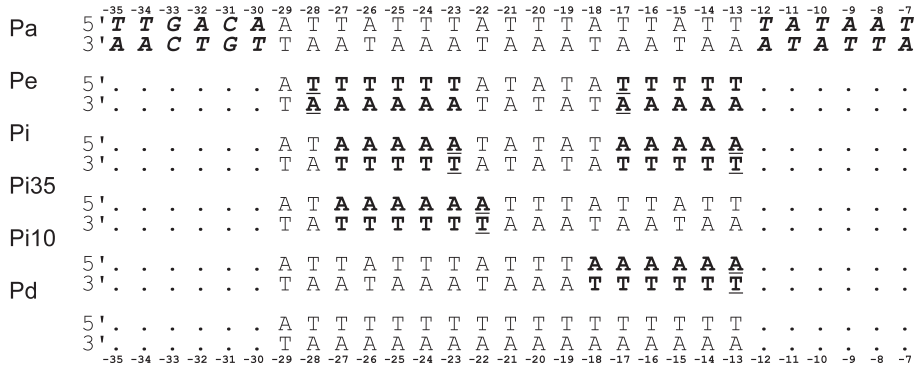

Figure 1. Sequences of the synthetic *Escherichia coli* promoter Pa and its derivatives Pe, Pi, Pi35 and Pi10 bearing A_n (n = 5 or 6) DNA bending tracts either in the template or in nontemplate strand of the 17 bp spacer region, and of promoter Pd having in the spacer the $A_{16}\cdot T_{16}$ B'-DNA fragment.

A-tracts in bold font with underlined 3'terminal base at which DNA minor groove attains the smallest width, consensus –35 and –10 elements in italic bold font.

investigated. For comparison purposes we included into the study also promoter Pd (Łoziński *et al.,* 1991) having in the spacer the $A_{16}\cdot T_{16}$ sequence of B'-DNA form (Nelson *et al.,* 1987). This promoter was used along with Pe and Pi in our earlier EMSA investigations on the effect of spacer sequence on the gross-structure of open transcription complex *in vitro* and promoter strength *in vivo* (Łoziński *et al.,* 1991; Łoziński & Wierzchowski, 1996). Here we present results of all these investigations and interpret the kinetic data obtained in relation to the most recent structural (Murakami *et al.,* 2002) and kinetic (Saecker *et al.,* 2002) models of transcription initiation.

MATERIALS AND METHODS

RNA polymerase. RNA polymerase (EC 2.7.7.6) was prepared from *E. coli* C600 strain according to Burgess *et al.* (1975) except that Sephacryl S300 was used instead of Bio-Gel A5m, and was kept in a storage buffer (50% glycerol, 100 mM NaCl, 10 mM Tris/HCl pH 7.9, 0.1 mM DTT). Quantitation of its activity according to Chamberlin *et al.* (1983) showed that 50% of the holoenzyme $E\sigma^{70}$ form was active. The enzyme concentrations reported here refer to its active holo form.

Promoters. *E. coli* model promoter Pa, made of the consensus –35 and –10 hexamers separated by a 17 bp spacer, and its derivatives bearing two phased A_n-tracts in the spacer region: Pe–A_6 in the template strand, and Pi–A_5 in the nontemplate strand, as well as Pd containing the $A_{16}\cdot T_{16}$ B'-DNA sequence in the spacer region, were those obtained and cloned into pDS3 earlier (Łoziński *et al.,* 1991; Łoziński & Wierzchowski, 1996). Promoters Pi10 and Pi35, with a single A_6-tract in the template strand located immediately upstream of the –10 element and downstream of the –35 one, respectively, were synthesized as complementary pairs of 47 base long oligomers with restriction sites at the ends for *Xho*I and *Eco*RI enzymes, and cloned into pDS3. The sequences of all these promoters are shown in Fig. 1. For studies on open complex formation, 226 bp long DNA fragments of pDS3 containing these promoters were obtained by PCR amplification with the use of appropriately designed primers and an Ampligene thermocycler. Concentrations of PAGE purified fragments were determined spectrophotometrically.

Reagents and chemicals. γ-ANS-UTP (γ-aminonaphthalene-sulfonate-UTP) was prepared and purified (Kolasa, 2001) according to Yarbrough *et al.* (1979). ANS was from Fluka. UTP, ApA , heparin and 1.0 M stock solution of $MgCl_2$ were purchased from Sigma. All other chemicals were also of reagent grade.

Fluorescence-detected abortive initiation (FDAI) assay of association kinetics. In this assay (Bertrand-Burggraff *et al.,* 1984; Suh *et al.,* 1992), we used γ-ANS-UTP as an elongating NTP and ApA as the initiating nucleotide, so that ApApUpU was the only abortive transcription product at all the promoters studied. The amount of fluorescent ANS-pyrophosphate liberated in the course of the reaction was measured spectrofluorimetrically. Reactions were initiated by addition of $E\sigma^{70}$ in solution at 35 ± 0.1°C to the reaction mixture held at the same temperature in a fluorimetric cuvette and fast mixing for about 15 s with a Pasteur capillary pipette. The abortive reaction was carried out in Hepes buffer (25 mM Hepes, pH 8.0, 100 mM $MgCl_2$, 1 mM DTT, 0.1 mg/ml BSA) at the following initial concentrations of the reactants: 0.45 mM ApA, 0.1 mM γ-ANS-UTP, 5 nM promoter DNA, 25–200 nM $E\sigma^{70}$. Fluorescence was excited at 360 nm and its intensity monitored at 500 nm for a period corresponding to at least 7 time constants (τ_{obs}) of the reaction. Data from 3–6 independent reactions at every $E\sigma^{70}$ concentration were analyzed simultaneously by a nonlinear least-squares weighted (fluorescence intensity fluctuations as weighting factors) fit to the function: $N = N_0 + Vt - V\tau_{obs}(1 - \exp(-t/\tau_{obs}))$, where N and N_0

are proportional to the fluorescence intensity amounts of the product per promoter at time t and $t = 0$, respectively, V is the final steady-state rate of abortive product synthesis (mole product per mole promoter per second), t – time (s), and $\tau_{obs} = 1/k_{obs}$, where k_{obs} is the observed first order rate constant. Standard errors of τ_{obs} were calculated using the Marquardt algorithm for minimization of χ^2. The steady- state rates (V) obtained in lag-assays at different enzyme concentrations for the same promoter under the same set of solution conditions agreed within ±10% with those determined in control reactions initiated by addition of ApA and γ-ANS-UTP to preformed open complexes. They proved independent of the initial enzyme concentration used in large excess relative to that of promoter DNA.

FDAI fixed-time assay of dissociation kinetics. To determine the rate constant of dissociation of the open complexes, k_d, the decrease in their original concentration was measured by the FDAI assay at various time intervals after addition of an excess of a polyanionic competitor heparin. The enzyme (50 nM) and promoter (10 nM) were preincubated in the Hepes reaction buffer containing 60–90 mM $MgCl_2$, for 30 min at 35°C. Heparin was added to a final concentration of 25 μg/ml, above which the reaction proved to be independent of the competitor content. Aliquots (200 μl) were removed before and at various times after heparin addition and placed in a temperature-equilibrated fluorescence couvette. FDAI steady-state reactions were initiated at 35°C by addition of the substrates in the Hepes buffer (50 μl) to the final concentration of 0.45 mM ApA and 0.1 mM γ-ANS-UTP, and the fluorescence intensity was measured as described above.

RESULTS

The aim of this work was to probe contacts between RNAP and promoter spacer region by insertion thereto of A-tracts of a structure different from the flanking B-DNA, characterized by decreasing width of the minor groove in the 5' → 3' direction and bends at both junctions (MacDonald *et al.*, 2001), and examination of effects of the induced perturbations in the structure of the open complex on the kinetics of abortive transcription *in vitro*.

The sequences of the parent Pa promoter and its derivatives designed for this study, having the bending A_n (n = 5 or 6) tracts variously located in their 17 bp spacer region, are depicted in Fig. 1. Promoter Pe bears in regions –28 ... –23 and –17...–13 of the template strand two A_6-tracts in phase with the helical repeat of B-DNA. In promoter Pi, two phased A_5-tracts are located in the nontemplate strand of the same spacer regions as in Pe. Promoters Pi35 and Pi10 bear only one A_6-tract in region –27...–22 or –18 ...–13 of the nontemplate strand, respectively. Note that the corresponding A-tracts in Pe and in the Pi group of promoters have opposite orientations, 3' → 5' and 5' → 3', respectively. In the Pd promoter, the long A_{16} stretch in the spacer is located in the template strand, like the two A_6-tracts in Pe, and is expected to impose on this DNA fragment the B'-DNA structure (Nelson *et al.*, 1987). Note that this stretch is actually longer, A_{17}, since it extends to A(–12) of the –10 recognition hexamer.

The kinetics of the open complex formation at these promoters by *E. coli* RNA polymerase holoenzyme was studied under assumption of the minimal three-step mechanism (Scheme 1), shown to be fully applicable to the parent Pa promoter (Kolasa *et al.*, 2001). According to this model (Tsodikov & Record, 1999), the first intermediate closed complex (I_1), remaining in rapid-equilibrium with RNA polymerase (R) and promoter DNA (P), undergoes isomerization to a long-lived intermediate (I_2) followed by DNA melting between the –10 element and transcription start point and formation of the open complex (RPo):

$$R + P \underset{k_{-1}}{\overset{k_1}{\leftrightarrow}} I_1 \underset{k_{-2}}{\overset{k_2}{\leftrightarrow}} I_2 \underset{k_{-3}}{\overset{k_3}{\leftrightarrow}} RPo \qquad \text{(Scheme 1).}$$

The observed pseudo first-order rate, $k_{obs} \equiv 1/\tau_{obs}$, of the transcription reaction is related to the composite second-order association rate constant k_a and the composite first-order isomerization rate constant k_i by Eqn. 1:

$$\tau_{obs} \equiv (k_{obs})^{-1} = (k_a\,[R]_T)^{-1} + (k_i)^{-1} \qquad (1),$$

where $[R]_T$ is the total concentration of active $E\sigma^{70}$ and τ_{obs} – a lag-time necessary to reach the steady-state by the transcription reaction. Provided that the association reaction exhibits at $[R]_T \geq 0.3\ k_i/k_a$ single-exponentiality, and the fraction of long-lived complexes approaches unity, then $k_i \approx k_2 << k_{-1}$ and $k_a = K_1 k_2$ (Tsodikov & Record, 1999). These parameters were determined by measuring τ_{obs} as a function of enzyme concentration using fluorescence-detected abortive initiation assay (FDAI) with γ-ANS-UTP as a substrate, described in Methods. Linear weighted least-squares fit of Eqn. 1 to the experimental τ_{obs} ($[R]_T$) data, plotted in Fig. 2, yielded k_a and k_i parameters, collected in Table 1. Using the k_a and k_i values obtained, the corresponding K_1 equilibrium constants were calculated (cf. Table 1). As it can be judged from the experimental data, the formulated conditions of single exponentiality were satisfactorily fulfilled.

For RPo at Pa, Pe and Pi the rates of their irreversible dissociation, k_d, in the presence of an excess of the polyanionic competitor heparin were also determined (cf. Methods) to calculate the respective overall equilibrium stability constants for the open complexes at these promoters: $Kp = k_a/k_d$ (Table 1). Measurements of this rate as a function of $MgCl_2$ concentration, shown (Tsodikov & Record, 1999) to be related to the pertinent microscopic parameters (cf. Scheme 1) as $k_d = k_{-2}(1+ K_3)^{-1}$, allowed us to determine the number, n(Mg), of Mg^{2+} ions, involved in ionic exchange reactions accompanying DNA renaturation and I_2 reisomerization (Suh *et al.*, 1992; Saecker *et al.*, 2002). From the slopes, Sk_d = n(Mg), of double-logarithmic plots of k_d *versus* $[MgCl_2]$, shown in Fig. 3, the following n(Mg) values were obtained: 3.6 (±0.3), 4.0 (±0.2) and 5.0 (±0.3) for the Pa, Pe and Pi promoters, respectively.

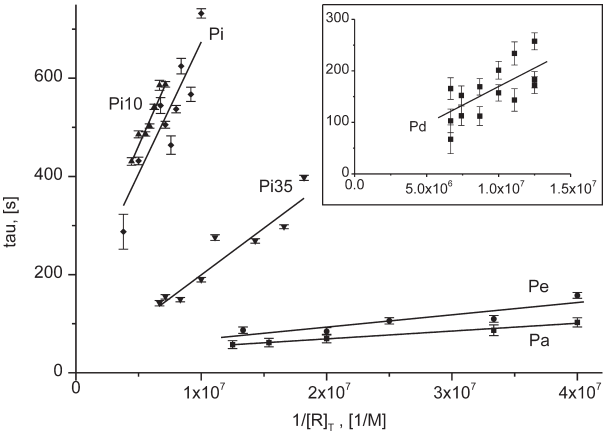

Figure 2. Kinetics of open complex formation.

Plots according to Eqn. 1 of experimental τ_{obs} data *vs.* 1/[RNAP] for Pa, Pe, Pi, Pi35 and Pi10 promoters, in Hepes buffer at 35°C; in the inset for promoter Pd under the same experimental conditions.

Comparison of the values of the k_a rate constant for open complex formation (Table 1) at the parent Pa promoter and at its two derivatives (bearing in the spacer region two similarly located but inversely oriented A-tracts) Pe and Pi, shows that at Pi the value of this parameter is strongly reduced, by a factor of 30, while that for Pe only by about 38%. This large reduction in the forward reaction rate at Pi is mainly due to an one order of magnitude smaller equilibrium binding constant K_1 and to an about four-fold lower isomerization rate constant k_i. The rate of RPo dissociation at this promoter appeared to be two-fold higher than at the parent Pa promoter, so that the calculated overall equilibrium constant Kp for RPo at Pi appeared to be reduced, relative to that at Pa, by a factor of 60. At the Pe promoter, the rate of the isomerization step is almost unaffected, hence the observed small decrease of k_a can be attributed solely to the proportionally smaller value of K_1. Since in

this case k_d was found somewhat lower, the calculated value of *K*p practically does not differ from that for RPo at Pa. The large difference in stabilization of RPo at Pa and Pe on the one hand, and at Pi on the other is also reflected in the number n(Mg) of Mg^{2+} ions rebound upon conversion of RPo to I_2 (cf. Fig. 3); in the case of Pa and Pe this number equals about 4, while in the case of Pi it is by one unit larger, i.e. 5. These numbers are equivalent to 7 and 9 monovalent cations, respectively, since 1.8 Na^+ ions become released upon binding of one Mg^{2+} to dsDNA (Misra & Draper, 1999).

Inspection of the kinetic parameters for promoters with only one of the two A-tracts present in the Pi promoter: Pi10 having the A_6 Pi10 promoters the rate constant for this step was found significantly, four-fold, lower. It is thus obvious that the effects of each of the two bending tracts on RPo formation at Pi are not additive.

The rate of RPo formation at the Pd promoter, having almost the whole spacer made of a stiff $A_{16}\cdot T_{16}$ B'-DNA fragment, was found also slowed down by one order of magnitude relative to that observed at the control Pa promoter (Table 1). Too large scatter of experimental data in the tau-plot (cf. inset to Fig. 2) did not allow, however, reliable evaluation of the k_i parameter, and hence also of K_1.

The large differences observed in the kinetics of abortive transcription initiation at the Pa, Pi and Pd promoters are not reflected in

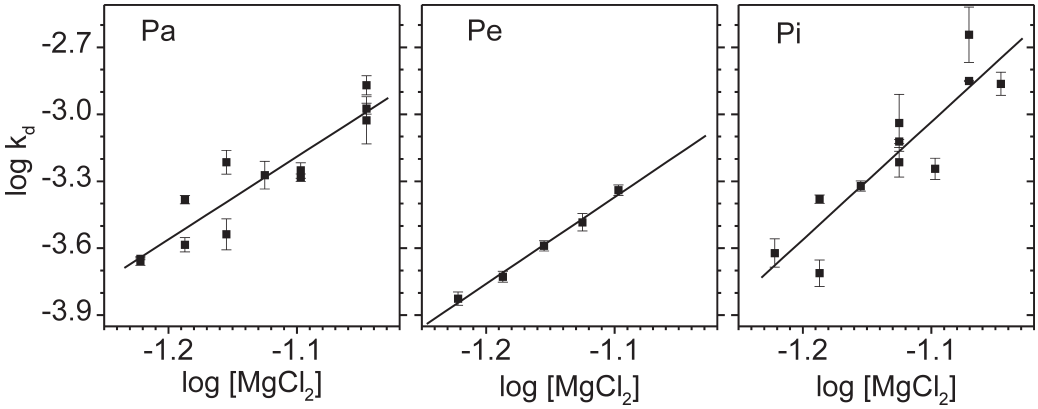

Figure 3. Double-logarithmic plot of the dissociation rate constant k_d of RPo at Pa, Pe and Pi promoters *vs* [$MgCl_2$].

Solid lines correspond to least squares fitted functions: (Pa) log k_d = 0.69(0.36) + 3.55(0.3), (Pe) log k_d = 1.01 (0.24) + 3.98 (0.21), (Pi) log k_d = 2.5 (0.35) + 5.00 (0.32); in brackets standard deviations at 0.95 confidence.

run at the –13...–18 location, and Pi35 with A_6 between positions –22 and –27, shows that the former run is sufficient to bring about a similar reduction of the k_a, K_1 and k_i parameters as do the two runs in Pi. The single A_6(–22 ...–27) sequence in Pi35 caused also a significant 10-fold decrease in the forward reaction rate, but smaller by a factor of 3 than A_6 at the –13/–18 location. It did not exert, however, any significant effect on the $I_1 \leftrightarrow I_2$ isomerization step since k_i at the Pi35 and Pa promoters can be regarded similar within the experimental error. At the Pi and the promoters' strength *in vivo* (cf. Table 1), determined previously by quantification of the amount of full-length RNA transcripts (Łoziński & Wierzchowski, 1996). This apparent discrepancy is most probably due to the control of transcription at the promoter escape and RNA elongation steps (Hsu, 2002), absent in the abortive experiments *in vitro*. It can be thus concluded that the effects of promoter structure perturbation should be rather probed at the early steps of transcription initiation.

Table 1. Kinetic parameters of open complex formation and dissociation at control promoter Pa and its derivatives in transcription buffer (25 mM Hepes, pH 8, 100 mM $MgCl_2$) at 35°C *in vitro* (in brackets standard deviations at 0.95 confidence), and strength *in vivo*.

Promoter	k_a (10^5 $M^{-1}s^{-1}$)	K_1 (10^7 M^{-1})	k_i (10^{-2} s^{-1})	k_d^a (10^{-3} s^{-1})	K_p (10^8 M^{-1})	Strength[b] (in *bla units*)
Pa	6.3(.3)	2.34(.01)	2.7(.2)	1.69(.32)	3.7(.5)	11.4
Pe	3.9(1.0)	1.69(.3)	2.3(1.0)	1.08(.08)	3.6(.7)	9.1
Pi10	0.17(.02)	0.29(.04)	0.59(.14)	–	–	
Pi35	0.63(.04)	0.17(.07)	3.65(1.7)	–	–	
Pi	0.19(.03)	0.25(.08)	0.7(.4)	3.17(.2)	0.06(.006)	8.2
Pd	0.63(1.65)	–	–	–	--	10.5

[a]Obtained by linear extrapolation from lower $MgCl_2$ concentrations using the fitted functions listed in the legend to Fig. 3.
[b]from Łoziński & Wierzchowski (1996).

DISCUSSION

The observed effects of insertion into the spacer region of the parent Pa promoter of A_n (n = 5 or 6) DNA bending tracts on the kinetics of open complex formation at its derivatives Pe, Pi, Pi35 and Pi10 (Table 1) are summarized in Scheme 2. Here, the changes in k_a

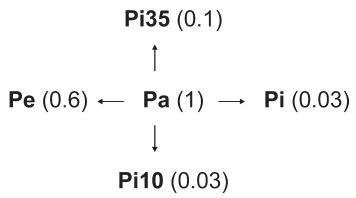

(Scheme 2)

are expressed as the ratio of this rate constant determined at a given promoter relative to that at Pa (numbers in parentheses). The most remarkable conclusion drawn from the experimental data is that A-tracts exert a profound down effect on the forward rate of RPo formation only when located in the nontemplate strand in either of the two spacer regions. The rate of open complex formation at Pe, bearing two A_6-tracts in the template strand, was found similar to that at the Pa promoter. We showed earlier (Łoziński & Wierzchowski, 1996; Kolasa, 2001) that the two bending tracts in Pe and in Pi, aligned in phase with B-DNA repeat, bend DNA axis in one plane (yz) similarly by about 40° to the outside of RNAP surface, while in the other plane (xz) this axis is only slightly bent in opposite directions: in Pe towards and in Pi to the outside of RNAP surface. All these observations indicate that the overall bending of DNA helical axis within the spacer DNA can not be held solely responsible for the very different kinetics of RPo formation at these promoters. The reasons for the observed drastic difference between the kinetics of RPo formation at Pa and Pe on one hand, and promoters Pi, Pi35 and Pi10 having A-tracts in the nontemplate DNA strand, on the other, should be thus sought in perturbation by these tracts of local DNA structure and, in turn, the interactions between RNAP and the spacer DNA in RPo. The control Pa promoter functions as a strong *E. coli* consensus-like promoter under both *in vivo* and *in vitro* conditions (Łoziński *et al.*, 1991; Łoziński & Wierzchowski, 1996; Kolasa, 2001; Kolasa *et al.*, 2002). Moreover, the spacer region in Pa is expected to be very flexible as made solely of AT base pairs with four interspersed TA

steps (Boutonnet *et al.*, 1993; Gorin *et al.*, 1995). Therefore, the protein–DNA interactions in the course of RPo formation at this promoter by RNAP can be considered close to optimal.

An insight into how an A-tract may perturb B-DNA structure is provided by the first long-range solution structure of an A_6-tract flanked by B-DNA fragments, solved by application of NMR spectroscopy with residual dipolar couplings (Mac Donald *et al.,* 2001). The A-tract itself has negative base inclination and a slight 5° bend towards the minor groove of the tract, the width of which narrows in the 5' to 3' direction by as much as about 5 Å. Due to the change in base inclination a large 10° bend occurs at the 3' junction, and a smaller one at the 5' junction, due to changes in the tilt and roll angles between adjacent base pairs. The structure of A_6 displays thus an overall bend of about 19° toward the minor groove. In the light of recent studies (Ross *et al.*, 2001; Yasuno *et al.*, 2001), it is this particular structure of the minor groove of A-tracts which confers sequence specificity in interactions between the CTD of RNAP α subunit and the UP promoter element. Namely, αCTD contacts DNA backbone from the minor groove which allows Arg265 guanidinum group of each of the two helix-hairpin-helix motifs of αCTD to interact with both sides of the negatively charged phosphate backbone most strongly within the narrowest part of the groove at its 3' end (Yasuno *et al.*, 2001). In regular B-DNA, amino acid–base contacts *via* the minor groove are made non-specifically since bases there have relatively similar van der Waals surfaces and similar hydrogen bond acceptors (O2 on purine and N3 on pyrimidine) (Luscombe & Thornton, 2002).

The sequence of the spacer in Pe promoter differs from that of the parent Pa only by two base pair replacements: A·T(–26) → T·A and A·T(–15) → T·A. Therefore, the pattern of the distribution of donor/acceptor groups of the bases in DNA grooves should be quite similar in both promoters. On the other hand, insertion in the same spacer regions of two phased A_5-tracts in the nontemplate strand of Pa, yielding promoter Pi, resulted in much more profound sequence differences between the two promoters and hence also in the pattern of donor/acceptor groups distribution in DNA grooves. The most significant difference between the two bent analogues Pe and Pi is the reverse orientation of the A-tracts, and thus also very different topology of the donor/acceptor groups in DNA grooves. Moreover, owing to the reverse orientation, the minor grooves of corresponding tracts attain the smallest width at opposite ends, which might additionally differentiate the protein–DNA interactions in the open complex formation. In the Pi35 and Pi10 promoters the single A_6-tracts have similar location as in Pi, except that they are longer by one base. However, neither this difference in the length nor the somewhat different flanking base sequences are likely to significantly influence the overall bending and structure of the minor groove in the A-tracts (MacDonald *et al.*, 2001).

How these expected perturbations in the spacer B-DNA structure by nontemplate A-tracts and their deleterious effects on the kinetics of transcription initiation can be interpreted in relation to the present model of RPo structure (Murakami *et al.*, 2002) and the structure-based kinetic model of its three-step formation (Saecker *et al.*, 2002) remains debatable.

According to the low resolution (6.5 Å) RPo model (Murakami *et al.*, 2002), based on the crystal structure of *Thermus aquaticus* RNAP complexed with a forked promoter template, the double stranded promoter DNA is anchored on the RNAP surface through major groove contacts of the –35 and –10 elements with σ^A regions 4 and 2, respectively, and just 5' of the –10 hexamer with amino acids of σ^A region 3, and DNA phosphates at positions –22 (template strand) and –27 (nontemplate strand) with the β' subunit NH_2-terminal

Zn^{2+}-binding domain (β'ZBD). These protein–DNA interactions induce in the spacer DNA two bends toward its major groove: (i) of about 8° centered at the –25 and (ii) of about 37° centered at the –16 position.

Remarkably, locations of the A-tracts in the studied group of promoters that perturb RPo function coincide with the two bent spacer regions in RPo. The location of the nontemplate $(-27)A_5(-23)$ and $(-27)A_6(-22)$ tracts in Pi an Pi35, respectively, as well as that of the template $(-28)A_6(-23)$ tract in the Pe promoter, coincides with the spacer region in contact with the β'ZBD domain. Apparently, in this spacer region of Pi and Pi35 the topology of the donor/acceptor groups exposed in the major DNA groove, the minimal width of the minor groove of the A-tracts close to their 3' ends at –23 or –22, and possibly also an about 19° bend towards the minor groove, centered similarly but in opposite direction than that caused by RNAP, do not allow accommodation of the β'ZBD domain in RPo as well as in Pa. In Pe, the pattern of potential protein- DNA contacts in the major groove can be expected to be similar to that in Pa, as discussed above, therefore the slightly slower kinetics of RPo formation at this promoter can be attributed to the somewhat higher energy of activation necessary to rearrange the unique structure of the bending tract to that of B-DNA required for a better fit.

The $(-17)A_5(-13)$ and $(-18)A_6(-13)$ nontemplate tracts of Pi and Pi10, respectively, lie in the –10 extended promoter region exhibiting a sharp 37° DNA bend toward the major groove, centered at –16 bp, and immediately adjacent to the –12 base pair forming the upstream edge of the melted DNA region. In the RPo structure (Murakami *et al.*, 2002), Gln^{260} of σ^A region 2.4 (corresponding to Gln^{437} of *E. coli* σ^{70}) could interact with the nontemplate strand T or the template strand A of this base pair. Moreover, a Trp residue of σ 2.3 region (Trp^{256} of *T. aquaticus*, corresponding to Trp^{433} of *E. coli* σ^{70}) is stacked against the –12 bp, downstream of which DNA strands become separated and take different paths while DNA undergoes two sharp 90° bends at the double-strand/single-strand junctions.

The –16 spacer region may also remain in contact with the 3.0 (formerly named 2.5) region of σ^{70} subunit, as indicated by the results of genetic mutational studies embracing both the DNA and the protein components of RPo (Fenton *et al.*, 2000; Sanderson *et al.*, 2003, and references therein). They have suggested occurrence of specific interaction between the side chains of some amino-acid residues (I^{439}, R^{441}, H^{455} and E^{458}) of this domain and the 5' TG 3' dinucleotide at the –14/–15 location in –10 extended promoters. In promoters lacking this TG motif, σ^{70} still may contact this promoter region, as shown by footprinting and crosslinking experiments (Schickor *et al.*, 1990; Mecsas *et al.*, 1991; Rudakova *et al.*, 2000; Naryshkin *et al.*, 2000; Studitsky *et al.*, 2001), but the DNA–protein interactions are expected to be less specific and weaker. All these data have indicated multiplicity of highly specific interactions of RNAP with DNA in the spacer region adjacent to the –10 element, involving regions 2.3, 2.4 and 3.0 of σ^{70}. These interactions, owing to their specificity, are likely to be strongly perturbed by the structure of the nontemplate A-tracts expected to impose the smallest width of the minor groove and the largest DNA bends at their 3' ends located at the –13 bp of the spacer.

Recent kinetic and thermodynamic studies of RNAP association with λP_R promoter (Saecker *et al.*, 2002) provided new insights into the development of RNAP–promoter contacts and allowed formulating a structural model of the kinetically significant intermediate I_1 on the pathway to RPo formation. They have demonstrated that the large and negative activation heat capacity of k_a, observed also previously (Roe *et al.*, 1984; 1985) and ascribed to I_2 formation, originates largely from formation of I_1 (cf. Scheme 1). In connection with the available structural and biochemical

data, the authors propose that formation of I_1 involves coupled folding of unstructured regions of RNAP and 90° kinking of promoter DNA at the –11/–12 base pairs that places the downstream DNA (–5 to +20) in the jaws of the β and β' subunits of RNAP (Murakami *et al.*, 2002; Mekler *et al.*, 2002). The subsequent slow conversion of I_1 to I_2 initiates separation of DNA strands from the –10 region to the start site and movement of the template strand down to the active site; it is accompanied by conformational transitions involving large changes in the exposure of polar and/or charged surfaces to water.

These interpretations seem to be generally applicable to the formation of transcription complexes at the parent Pa promoter and its derivatives bearing A-tracts because the kinetic, thermodynamic, and ionic characteristics of RPo formation at Pa and λP_R have been shown to be similar (Kolasa *et al.*, 2001). From this perspective, the nontemplate (–27)A_5(–23) or (–27)A_6(–22) tracts of Pi and Pi35, shown to induce a large decrease in the equilibrium constant K_1, perturb mostly the coupled conformational changes in RNAP and DNA leading to formation of I_1. The nontemplate tracts (–17)A_5(–13) of Pi and (–18)A_6(–13) of Pi10 decreasing both K_1 and k_i , and increasing k_d by a factor of about 2 in the case of Pi, affect thus both the formation of I_1 as well as the subsequent conformational processes of its isomerization to I_2. The expected large free energy cost of a 90° DNA deformation at the –11/–12 bp (Saecker *et al.*, 2002) should be thus significantly increased to overcome the perturbation of promoter structure by this A-tract. The larger number of Mg^{2+} ions found to be in control of the dissociation of RPo at Pi indicates that presence of the (–17)A_5(–13)-tract influences the postulated coupled ionic exchange processes.

The 17 bp long B'-DNA fragment in promoter Pd has the A_{17} -tract located in the template strand, like the two A_6-tracts in Pe. Therefore, the topology of the acceptor/donor binding sites in DNA grooves of the two promoters can be expected to be generally similar, except for small differences in their spatial disposition due to the propeller twist of the A:T base pairs and the shortening by about 0.5 bp of the helical repeat of the spacer DNA (Nelson *et al.*, 1987) in Pd. The observed one order of magnitude slower forward rate of open complex formation at Pd seems thus to be connected rather with the stiffness of spacer B'- DNA (Nelson *et al.*, 1987). RNAP is able to bind promoters of different length, 17 ±1, by kinking DNA over a bulge in β' that intervenes between the regions 4 and 2 of σ^{70} involved in recognition of the –35 and –10 hexamers. It has been shown that increased flexibility of the spacer DNA caused by missing bases leads to increased promoter activity (Noel & Reznikoff, 2000). Conversely, the stiffness imposed on the spacer by the B'-DNA form should make its proper accommodation on the RNAP surface more difficult.

The strong down effects on the rate of open complex formation by A-tracts located in the template strand in either of the two spacer regions in contact with RNAP found in this work should be helpful in further elucidation of the nature of specific protein–DNA interactions in connection with higher-resolution structural data on RNAP–promoter complexes, expected to become soon available.

REFERENCES

Bertrand-Burggraf E, Lefévre JF, Daune M. (1984) A new experimental approach for studying the association between RNA polymerase and the *tet* promoter of pBR322. *Nucleic Acids Res.*; **12**: 1697–706.

Boutonnet N, Hui X, Zakrzewska K. (1993) Looking into the grooves of DNA. *Biopolymers.*; **33**: 479–90.

Burgess RR, Jendrisak JJ. (1975) A procedure for the rapid, large-scale purification of *Escherichia coli* DNA-dependent RNA polymerase involving Polymin P precipitation and

DNA-cellulose chromatography. *Biochemistry.*; **14**: 4634–8.

Chamberlin M, Kingston R, Gilman M, Wiggs J, deVera A. (1983) Isolation of bacterial and bacteriophage RNA polymerases and their use in synthesis of RNA *in vitro*. *Methods Enzymol.*; **101**: 540–68.

Chen H, Tang H, Ebright RH. (2003) Functional interaction between RNA polymerase alpha subunit C-terminal domain and sigma70 with UP-element- and activator-dependent transcription. *Mol Cell.*; **11**: 1621–33.

Estrem ST, Ross W, Gaal T, Chen ZW, Niu W, Ebright RH. (1999) Bacterial promoter architecture: subsite structure of UP elements and interaction with the carboxy-terminal domain of the RNA polymerase α subunit. *Genes Dev.;* **13**: 2134–47.

Fenton MS, Lee SJ, Graala JD. (2000) *Escherichia coli* promoter opening and –10 recognition: mutational analysis of σ^{70}. *EMBO J.*; **19**: 1130–7.

Gorin AA, Zhurkin VB, Olson W. (1995) B-DNA twisting correlates with base-pair morphology. *J Mol Biol.*; **247**: 34–48.

Hsu L. (2002) Promoter clearance and escape in prokaryotes. *Biochim Biophys Acta.*; **1577**: 191–207.

Kolasa IK. (2001) Influence of $A_n \cdot T_n$ DNA bending sequences on *Escherichia coli* promoter strength *in vitro*. *Ph.D. Thesis*, Institute of Biochemistry and Biophysics, Polish Academy of Sciences, Warszawa, Poland (in Polish).

Kolasa IK, Łoziński T, Wierzchowski KL. (2002) Effect of A_n tracts within the UP element proximal subsite of a model promoter on kinetics of open complex formation by *Escherichia coli* RNA polymerase. *Acta Biochim Polon.*; **49**: 659–69.

Luscombe NM, Thornton JM. (2002) Protein–DNA interaction: amino-acid conservation and the effects of mutations on binding specificity. *J Mol Biol.*; **320**: 991–1009.

Łoziński T, Wierzchowski KL. (1996) Effect of reversed orientation and length of $A_n \cdot T_n$ DNA bending sequences in the –35 and spacer domains of a consensus-like *Escherichia coli* promoter on its strength *in vivo* and gross structure of the open complex *in vitro*. *Acta Biochim Polon.*; **43**: 265–80.

Łoziński T, Adrych-Rożek K, Markiewicz WT, Wierzchowski KL. (1991) Effect of DNA bending in various regions of the consensus-like *Escherichia coli* promoter on its strength *in vivo* and structure of the open complex *in vitro*. *Nucleic Acids Res.*; **19**: 2947–53.

MacDonald D, Herbert K, Zhang X, Pologruto T, Lu P. (2001) Solution structure of an A-tract DNA bend. *J Mol Biol.*; **306**: 1081–98.

Mecsas J, Cowing DW, Gross CA. (1991) Development of RNA polymerase-promoter contacts during open complex formation. *J Mol Biol.*; **220**: 585–97.

Mekler V, Kortkhonija K, Mukhopadhyay J, Knight J, Revyakin A, Kapanidis AN, Niu W, Ebright YW, Levy R, Ebright RH. (2002) Structural organization of bacterial RNA polymerase holoenzyme and the RNA polymerase-promoter open complex. *Cell.*; **108**, 599–614.

Misra VK, Draper DE. (1999) The interpretation of Mg^{2+} binding isotherms for nucleic acids using Poisson-Boltzmann theory. *J Mol Biol.*; **294**: 1135–47.

Murakami KS, Masuda S, Campbell E, Muzzin O, Darst SA. (2002) Structural basis of transcription initiation: an RNA polymerase holoenzyme-DNA complex. *Science.*; **296**: 1285–90.

Naryshkin N, Revyakin A, Kim Y, Mekler V, Ebright RH. (2000) Structural organization of the RNA polymerase-promotor open complex. *Cell.*; **101**: 601–11.

Nelson HCM, Finch JT, Luisi BF, Klug A. (1987) The structure of an oligo(dA)·oligo(dT) tract and its biological implications. *Nature* (*London*).; **330**: 305–17.

Noel RJ, Reznikoff WS. (2000) Structural studies of *lac*UV5–RNA polymerase interactions *in vitro*. *J Biol Chem.*; **275**: 2708–12.

Roe J-H, Burgess RR, Record MT Jr. (1984) Kinetics and mechanism of the interaction of *Escherichia coli* RNA polymerase with the λP_R promoter. *J Mol Biol.*; **176**: 495–521.

Roe J-H, Burgess RR, Record MT Jr. (1985) Temperature dependence of the rate constants of the *Escherichia coli* RNA polymerase-λP_R promoter interaction. Assignment of the kinetic steps corresponding to protein conformational change and DNA opening. *J Mol Biol.*; **184**: 441–53.

Ross W, Ernst A, Gourse RL. (2001) Fine structure of *E. coli* RNA polymerase-promoter interactions: α subunit binding to the UP element minor groove. *Genes Dev.*; **15**: 491–506.

Ross W, Schneider DA, Paul BJ, Mertens A, Gourse RL. (2003) An intersubunit contact stimulating transcription initiation by *E. coli* RNA polymerase: interaction of the α C-terminal domain and σ region 4. *Genes Dev.*; **17**: 1293–307.

Rudakova EA, Ivanovskaya MG, Kozlov MV, Khorotonenko MV, Oretskaya TS, Nikiforov VG. (2000) Probing of contacts of oligonucleotide phosphate groups from the non-template strand of *lac*UV5 promoter with RNA polymerase of *E. coli* by regioselective crosslinking. *Biokhimija.*; **65**: 753–64.

Saecker RM, Tsodikov OV, McQuade KL, Schlax PE Jr, Capp MW, Record MT Jr. (2002) Kinetic studies and structural models of the association of *E. coli* σ^{70} RNA polymerase with the λP_R promoter: large scale conformational changes in forming the kinetically significant intermediates. *J Mol Biol.*; **319**: 649–71.

Sanderson A, Mitchell JE, Minchin SD, Busby JW. (2003) Substitutions in *Escherichia coli* RNA polymerase σ^{70} factor that affect recognition of extended –10 elements at promoters. *FEBS Lett.*; **544**: 199–205.

Schickor P, Metzger W, Werel W, Lederer H, Heumann H. (1990) Topography of intermediates in transcription initiation of *E. coli*. *EMBO J.*; **9**: 2215–20.

Studitsky VM, Brodolin KL, Liu Y, Mirzabekov AD. (2001) Topography of *lac*UV5 initiation complexes. *Nucleic Acids Res.*; **29**: 854–61.

Suh WC, Leirmo S, Record MT Jr. (1992) Role of Mg^{2+} in the mechanism of formation and dissociation of open complexes between *Escherichia coli* RNA polymerase and the λP_R promoter: Kinetic evidence for a second open complex requiring Mg^{2+}. *Biochemistry.*; **31**: 7815–25.

Travers AA. (1987) Structure and function of *E. coli* promoter DNA. *CRC Crit Rev Biochem.*; **22**: 181–219.

Tsodikov OV, Record MT Jr. (1999) General method of analysis of kinetic equations for multistep reversible mechanisms in the single-exponential regime: Application to kinetics of open complex formation between Eσ^{70} RNA polymerase and λP_R promoter DNA. *Biophysical J.*; **76**: 1320–9.

Yarbrough LR, Schlageck JG, Baughman M. (1979) Synthesis and properties of fluorescent nucleotide substrates for DNA-dependent RNA polymerases. *J Biol Chem.*; **254**: 12069–73.

Yasuno K, Yamazaki T, Tanaka Y, Kodama TS, Matsugami A, Katahira M, Ishihama A, Kyogoku Y. (2001) Interaction of the C-terminal domain of the *E. coli* polymerase α subunit with the UP element: recognizing the backbone structure in the minor groove surface. *J Mol Biol.*; **306**: 213–25.